Journal of Thermal Analysis and Calorimetry (2022) 147:10403–10409
https://doi.org/10.1007/s10973-022-11253-3

Dose-dependent effect of cyclophosphamide treatment on actin

Dénes Lőrinczy[1] · **Dávid Szatmári**[1]

Received: 17 November 2021 / Accepted: 27 January 2022 / Published online: 21 February 2022

Abstract
The actin is the essential unit protein of cytoskeleton and muscle sarcomeres. The continuous management of filaments is the key machinery of eukaryotic cytoskeletal plasticity which based on the different complexes with divalent cations (Ca^{2+} or Mg^{2+}) and nucleotides (ATP, ADP). Any structural modification of nucleotide-binding sites in G actin can bind ATP or ADP under different cation conditions and can initialize the remodelling of the cleft and change the stiffness of two main domains. The evolutionary important nucleotide-binding cleft as a bridge between the two domains needs more investigation to can express its importance in the development of actin functions. The cyclophosphamide (CP) is a cytostatic drug applied in chemotherapy it can alkylate the long residues in the ATP binding sites thus change the structure of the binding cleft. Our previous study explained that the actin filaments show less sensitivity to the CP treatment than monomers. Here we investigate the CP dose-response effect on the thermodynamic stability of actin monomers and polymers in the presence of Ca^{2+} or Mg^{2+} to know the minimum effective concentration for the interpretation of any relevant dosage at level of tissues. The previously expressed "titled state" EM model of filamentous actin based on the same structural change of monomers as we found here where the domains react to any modification with taking apart sd4 from sd2 results in a more exposed nucleotide-binding cleft.

Keywords Cyclophosphamide dose · Actin · DSC · Thermodynamics

Introduction

The eukaryotic cytoskeletal system is a dynamical scaffold based on different proteins [1]. The actin is the essential unit protein of cytoskeleton and muscle sarcomeres [2–4]. Different states of forming filaments (F actin) from monomeric actin (G actin) are implicated in cell motility, transport processes and cell division [5–11]. The management of actin filaments is the key machinery of eukaryotic cytoskeletal plasticity which based on the different complexes with divalent cations (Ca^{2+} or Mg^{2+}) and nucleotides (ATP, ADP) [12–21]. Cation and nucleotide-binding regulates the structural stability of actin monomers but the form that is bound to ATP is more frequent in cells when actin is in monomer state [21, 22]. With the actin polymerization the ATP is hydrolysing to ADP [13–22]. Any structural modification of nucleotide-binding cleft in G actin which can bind ATP or ADP under different cation conditions can initialize the remodelling of the cleft and change the stability of two main domains [23–25]. Nearby of filaments Mg^{2+} and Ca^{2+} conditions can rearrange the ATP binding of motor proteins and actin maintaining proteins [26, 27]. Previous studies expressed the importance of activation energy according to the thermal stability of domains that enhanced kinetics of domains belongs to a more advantageous case of protein structural plasticity and shows significant reaction to different cations and nucleotides [27–31].

The cyclophosphamide (CP) is a cytostatic drug applied in chemotherapy [32–38]. Previous studies has been shown with deconvolution of collected DSC scan data that there is a possible effect in Guinea pig and rabbit muscle fibres on the level of actin or myosin [38–42]. The ligand binding on actin filaments is usually cooperative and enhances allosteric conformational change along the filament [43–47]. Jasplakinolide and phalloidine toxins are binding to actin and induce concentration-dependent cooperative effect on actin [48, 49]. Previous studies shown [39, 40, 50] that muscle

Dénes Lőrinczy and Dávid Szatmári have contributed equally to this work.

✉ Dénes Lőrinczy
denes.lorinczy@aok.pte.hu

[1] Department of Biophysics, Medical School, University of Pécs, Szigeti str. 12, Pecs 7624, Hungary

filament can be changed directly by the CP treatment [51]. The evolutionary important nucleotide-binding site as a bridge between the two domains links the structural integrity to the development of actin functions together [52–56]. This linker between the two major domains is based on the chain at residue Lys336 and the helix Gln137-Ser145 which plays the role as an axis and forms two clefts between the domains and due to the fact that Gln137 is a nucleotide-binding residue it can have effect on the linker with a modified interdomain flexibility [57, 58]. The upper cleft binds nucleotide and divalent cations which work together to provide another important linkage between domains. The structure of actin can be divided into four subdomains (sd1-4). The lower cleft between sd1 and sd3 contains mainly hydrophobic residues Tyr143, Ala144, Gly146, Thr148, Gly168, Ile341, Ile345, Leu346, Leu349, Thr351, and Met355. The Ser14 loop in sd1 and the loop containing Asp157 in sd3 are equivalent and binding the phosphates of the nucleotide [59]. Sd1 and sd3 can be described as a rigid core of the monomer [60]. Divalent cation binding residues (sd1: Glu361, Trp356, Gln354; sd2: Glu57, Arg62; sd3: Glu167, Gln263, Ser265, Asp286, Asp288; sd4: Ser199, Thr201, Glu205) are implicated in structural dynamics of subdomains [61]. The transition of G- to F-actin is propeller-like rotation of sd1-2 with flattening to the sd3-4 around an axis roughly at right angle to the helix axis [62]. On the subdomains, magnesium ions are able to bind in the same position as calcium thus by the higher number of Mg^{2+} coordinated residues increases the stiffness of actin filaments and results a buried structure and lower responsibility of sd3-4 [61]. The stiffness of the filaments depends on the Ca^{2+} or Mg^{2+} binding to a high-affinity site on sd2 (Gly36-Glu57) [58]. Nucleotide-dependent conformational changes with chain of Ser14 and the loop carrying His73 reacting to the state of the bound nucleotide [62]. However, sd4 is more flexible by the helix with residues of 223–230 and the loop with residues of 241–247 than sd2. With high number of helices and loops in sd2 can be provided an increased dynamical response to influences [60]. All the residues which are implicated in nucleotide-binding are well charged and keep on the thermal stability of the cleft thus balancing the structural dynamics of actin monomers. Complexes of nucleotides and cations make a bridge between sd1 and sd3 to form a stiff core with two flexible extensions as sd2 and sd4. Structural stiffness of sd2 and sd4 linked to the nucleotide binding core but mainly depends on did they bind Ca^{2+} or Mg^{2+} [61]. The mutation of residues or alkylation by CP in the binding cleft can change the structure of actin monomers with the protection and cover of ATP binding at methylated His73 or mutated His73Ala, Arg177Asp, Ser14Cys or Ser14Cys/Asp157Ala can lack ATP binding and enhances the nucleotide exchange [63–67]. As we have investigated, actin monomers are more sensitive to the CP treatment than filaments [57]. The heat stability of actin monomers and filaments as a response to the applied CP dose is not studied yet. Here we investigate the heat stability response of actin to increases concentration of CP in the presence of Ca^{2+} or Mg^{2+} to know the minimum effective concentration to can interpret any relevant dosage at level of tissues.

Materials and methods

Actin preparation from rabbit skeletal muscle

G and F-actin with Ca^{2+} or Mg^{2+} cations were prepared in the usual way from acetone powder of rabbit skeletal muscle as described earlier by Spudich and Watt [44], and stored in MOPS-buffer (2 mM MOPS, 0.2 mM ATP, 0.1 mM $CaCl_2$, 0.1 mM β-mercaptoethanol, pH 7.4). Actin concentration was determined from the absorption spectra (Jasco V-550 spectrophotometer, as the average concentration by $\varepsilon = 1.11$ mL mg^{-1}cm at 280 nm and $\varepsilon = 0.63$ mL mg^{-1}cm at 290 nm). We applied 2 mM EGTA then 2 mM $MgCl_2$ treatment for exchange calcium to magnesium on 2 mg mL^{-1} actin monomers, this way we remained close to the physiological concentration of actin. Actin polymerization process was initialized by addition of 100 mM KCl follow the same protocol as in our previous study [51, 57].

Cyclophosphamide treatment

In our, in vitro measurements, the applied dosage of cyclophosphamide (CP) was the same as the human dosage (150 mg kg^{-1} b.m.) during chemotherapeutic treatments [7–10]. The average actin content of skeletal muscle is roughly 10% of the actual muscle mass [44] thus the average mass of Guinea pig gastrocnemius muscle (from our previous study [8]) divided by 10 then by the mass of CP passed in the muscle [150 mg $kg^{-1} \times (m_{gastrocnemius}/m_{body})$]. The single-dose clearance with the circulation system depends on the total volume of blood and the adsorption rate between the plasma and the cells. Supposedly the adsorption rate is slower than the heart rate, so we can focus on only the blood circulation caused dilution and distribution in the whole body results that the actin to CP ratio can be use as 2000/3 (it means 2 mg actin to 3 μg CP) [51, 57]. However, as we used actin from rabbit skeletal muscle we can assume that the distribution of CP in rabbit skeletal muscle should be the same as in Guinea pig skeletal muscle. To achieve a more pronounced effect we carried out our experiments with 1, 3, 5 times conventional dose, 3 μg mL^{-1}, 9 μg mL^{-1}, 15 μg mL^{-1} of CP, respectively, to treat actin followed by incubation at room temperature for 1 h (in case of model experiment the animal underwent to a real, long-lasting chemotherapeutic protocol as described in [38–40, 50]).

DSC measurements

The actin samples with 2 mg mL^{-1} concentration were freshly prepared before all measurements. The analysis was made by a SETARAM Micro-DSCII calorimeter between 0 and 100 °C with heating rate of 0.3 K min^{-1}. Conventional Hastelloy batch vessels ($V_{max} = 1$ mL) were used for the experiment to investigate denaturation with 950 µL sample volume on average. Samples' masses were between 920 and 970 mgs. MOPS buffer was used as a reference. The reference and sample vessels were equilibrated with a precision of ± 0.1 mg; this way we did not need to do any correction between vessels' heat capacity. With the help of a two-point SETARAM peak integration setting, calorimetric enthalpy was calculated from the area under the heat absorption curve, and then, the results [denaturation or melting temperature (T_m) and calorimetric enthalpy (ΔH_{cal}) data of samples] were compared. This method is identical to the protocol as we applied in our previous study [51, 57].

Results

Figure 1 shows the thermal denaturation curves of G or F-actin in the presence of 2 mM $CaCl_2$ or 2 mM $MgCl_2$ were measured under different CP concentrations (0 µg mL^{-1}—black line, 3 µg mL^{-1}—red line, 9 µg mL^{-1}—blue line, 15 µg mL^{-1}—green line). On the basis of accurate analysis 3 µg mL^{-1} CP already modified the heat-response curves of actin-related to a structural change of distinct subdomains which is in a good agreement with our previous results [51]. The DSC scan of actin seems as the superposed response of four subdomains which was decayed to the components in the presence of CP. The Ca^{2+} or Mg^{2+} bound G or F-actin forms provide different sensitivity to CP treatment. In case

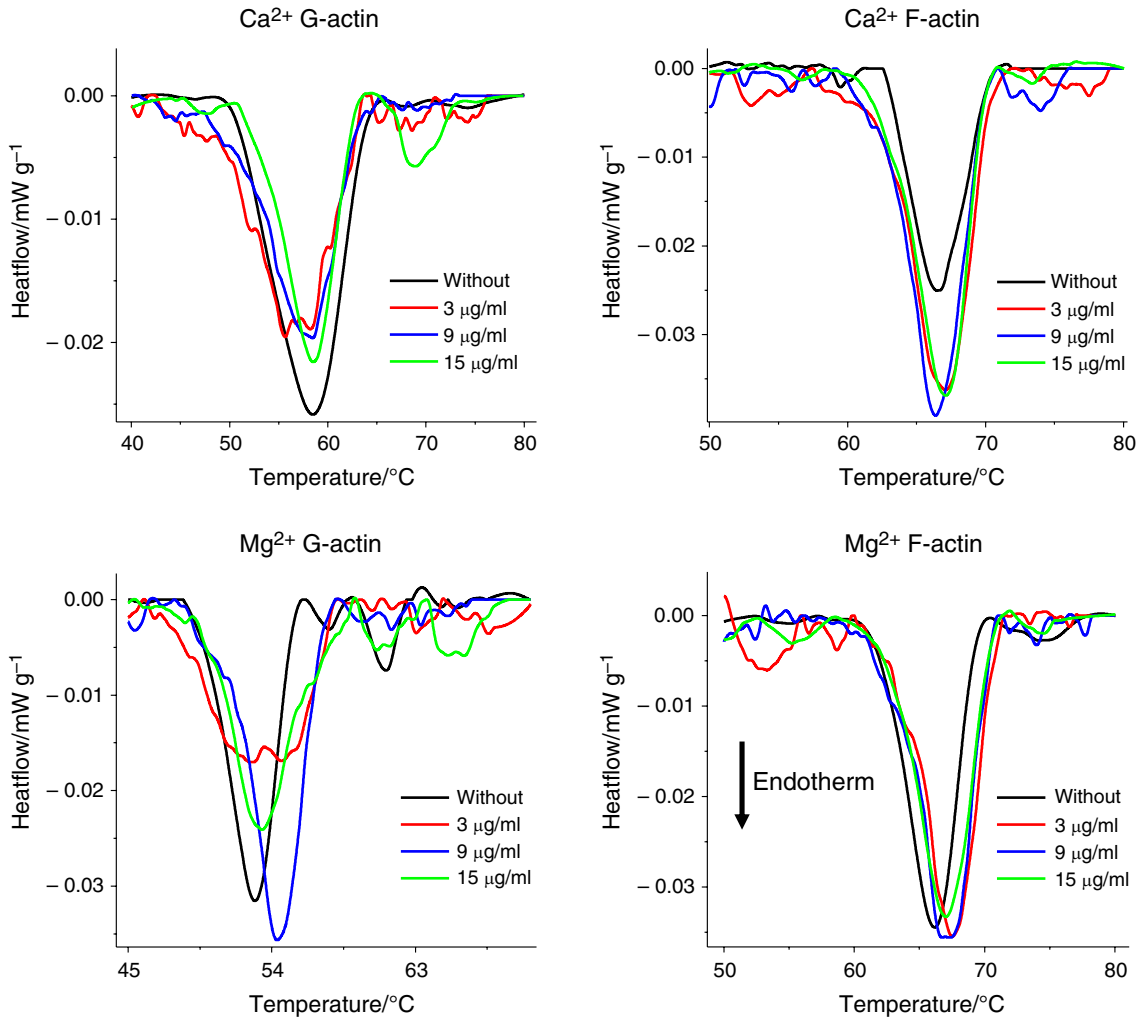

Fig. 1 Thermal denaturation curves of different G and F-actin in the absence (black line) and in the presence of different CP concentrations (3 µg mL^{-1}—red, 9 µg mL^{-1}—blue, 15 µg mL^{-1}—green line, endotherm effect is deflected downwards). (Color figure online)

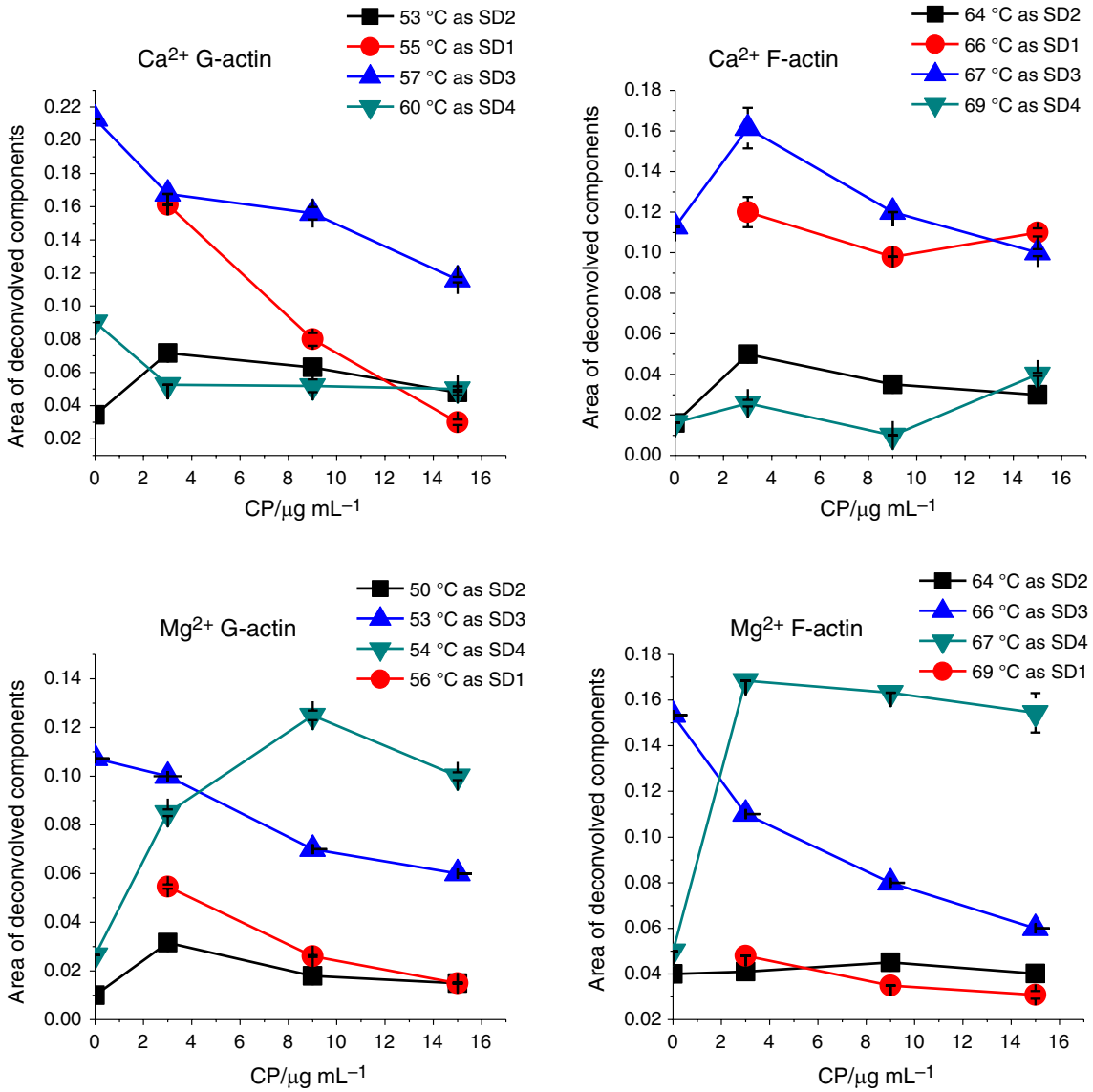

Fig. 2 Dose-response effects of CP on actin subdomains as the deconvolved components of DSC scans. The data presented were derived from at least 3 independent experiments. Values are displayed as the mean ± standard deviation

of filaments, heat response curves show less number of components than in case of monomeric actin.

Figure 2 shows the results after the deconvolution of DSC scan curves from Fig. 1 as CP concentration-dependent area change of deconvolved components related to the dynamics of each subdomain respectively.

In the absence of CP, there are only three components of the DSC graphs the two tiny peaks are the response of sd2 and sd4 subdomains which are linked to the sd1-3 core unit as the main peak. In the presence of CP, the DSC graphs contain one more peak seems like the response of sd1-3 core decayed to two components refers to a freely opened structure of the lower cleft by a possible alkylation of nucleotide-binding residues [63–67]. Small peaks at the lowest temperature level on each graph have to be the response of the simplest sd2 subdomain [60]. The flexibility of the sd4 depends on which type of cation binds to the high-affinity sites presumably Mg^{2+} can coordinate more residues than Ca^{2+} thus can dominate the heat response of actin [21, 59]. In case of Ca^{2+} G-actin, the area of peaks related to sd1-3 core unit decreases by CP in a concentration-dependent manner while other peaks related to sd2 and sd4 are seems independent of CP treatment. In case of Ca^{2+} F-actin, the area of peaks related to sd1-3 core unit and the two more peaks do not show any response to increases concentration of CP. In case of Mg^{2+} G-actin, the area of peaks related to sd1-3 core unit also decreases by CP in a concentration-dependent manner while the peak of sd4 turned to be the

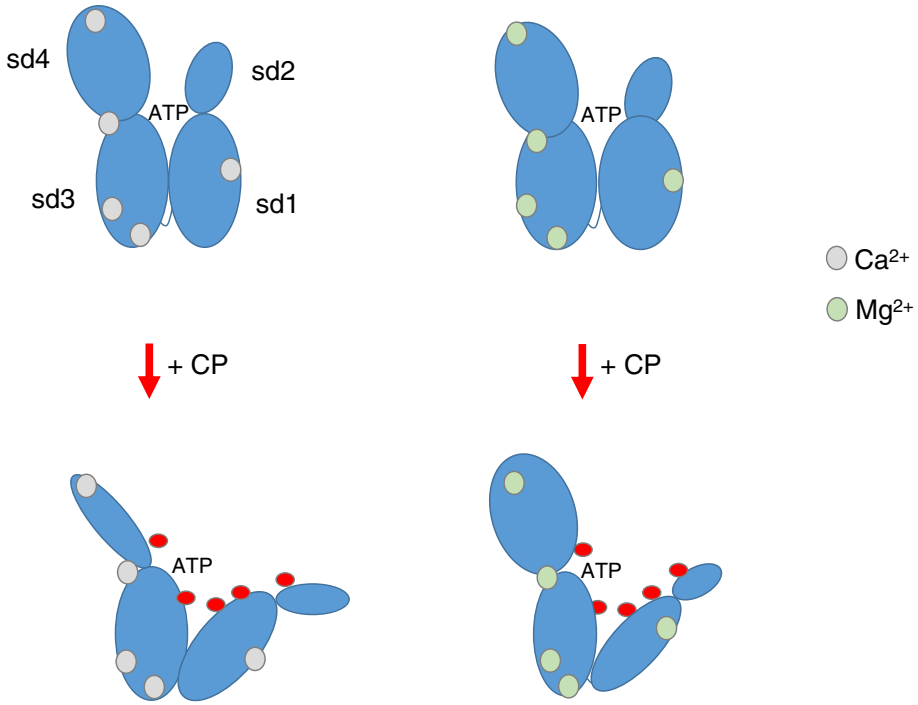

Fig. 3 Butterfly-like model: To explain the structural change of monomers as we found here where the domains react to CP treatment by taking apart sd4 from sd2 and open up the cleft between the two main domains with different structural dynamics of Ca^{2+} or Mg^{2+} bound subdomains

main component and the peak of sd2 seems independent of CP concentration. In case of Mg^{2+} F-actin, the area of peaks of sd1-3 core unit also decreases by CP in a concentration-dependent manner while the peak of sd4 turned out to be the main component already by 3 µg/ml of CP and the peak of sd2 still does not show any effect of CP.

Discussion

Ca^{2+} and Mg^{2+} can bind to the low and high-affinity cation binding sites on actin in the nucleotide-binding cleft and several more points on the surface of monomer [21]. Ca^{2+} can coordinate lower number of residues than Mg^{2+} with a lower affinity of nucleotide in the binding cleft results a more flexible composition of subdomains [61]. The CP treatment caused alkylation of nucleotide-binding residues can open up the lower and within the upper cleft of actin monomers and the "scissor-like" motion of domains can be transformed to a “butterfly-like” motion in a CP concentration dependent manner (Fig. 3). The previously expressed “titled state” EM model of filamentous actin based on the same structural change of monomers as we found here were the domains response to any modification with taking apart sd4 from sd2 results in a more exposed cleft between the two main domains [68]. The sd4 seems the most rigid basis of the Mg^{2+} bound highly dynamical alkylated structure of actin. In the axis of filamentous actin sd3-4 subdomains are buried and sd1-2 are more exposed to the environment [61]. Ca^{2+} bound actin monomers were stacked in a highly flexible filamental form which looks protected from the effect of CP while Mg^{2+} bound sd1-2 subdomains are moving freely on a stiff sd3-4 based filamental axis after CP treatment.

Conclusions

As it was expected [38–42] our recent study showed the importance of a single dose of CP (3 µg CP to 2 mg actin [51]) already can have effect on Guinea pig and rabbit muscle fibres. Ligand binding to actin modifies the structure of nucleotide-binding cleft and seems cooperative with an induced allosteric conformational change in the structure of actin filaments [43–47] with modified contractility of sarcomeres.

Acknowledgments This work was supported by CO-272 (OTKA) Grant (D.L.).

Author contributions DL: corresponding author, principle investigator, DSC experiments, data analysis, manuscript writing. DS: corresponding author, sample preparation and handling, data analysis, manuscript writing.

Funding Open access funding provided by University of Pécs.

Declarations

Conflict of interest The authors declare that they have no known competing financial interests or personal relationships that could have appeared to influence the work reported in this paper.

Consent for publication Copyright form has been uploaded with the manuscript.

References

1. Hardin J, Bertoni G, Kleinsmith LJ. Becker's world of the cell. 8th ed. New York: Pearson; 2015. p. 422–46.
2. Ono S. Dynamic regulation of sarcomeric actin filaments in striated muscle. Cytoskeleton. 2010;67:677–92.
3. Sanger JW, Wang J, Fan Y, White J, Mi-Mi L, Dube DK, et56 al. Assembly and maintenance of myofibrils in striated muscle. Handb Exp Pharmacol. 2017; pp. 39–75.
4. Gunning PW, Ghoshdastider U, Whitaker S, Popp D, Robinson RC. The evolution of compositionally and functionally distinct actin filaments. J Cell Sci. 2015;128:2009–19.
5. Cossart P. Actin-based bacterial motility. Curr Opin Cell Biol. 1996;7:94–101.
6. Steinmetz MO, Stoffler D, Hoenger A, Bremer A, Aebi U. Actin: From cell biology to atomic detail. J Struct Biol. 1997;119:295–320.
7. Pollard TD, Blanchoin L, Mullins RD. Molecular mechanisms controlling actin filament dynamics in nonmuscle cells. Ann Rev Biophys Biomol Struct. 2000;29:545–76.
8. Pollard TD, Borisy GG. Cellular motility driven assembly and dissembly of actin filaments. Cell. 2003;112:453–65.
9. Carlier M-F, Le Clainche C, Wiesner S, Pantolini D. Actin-based motility: From molecules to movement. BioEss. 2003;25:336–45.
10. Pantolini D, Le Clainche C, Carlier M-F. Mechanism of actin-based motility. Science. 2001;292:1502–6.
11. Hehnly H, Stamnes M. Regulating cytoskeleton-based vesicle motility. FEBS L. 2007;581:2112–8.
12. Sheterline P, Clayton J, Sparrow J. Actin. Prot Profile. 1995;2:1–103.
13. Feuer G, Molnár F, Pettko E, Straub FB. Studies on the composition and polymerization of actin. Hung Acta Physiol. 1948;1(4–5):150–63.
14. Pollard TD. Rate constants for the reactions of ATP- and ADP-actin with the ends of actin filaments. J Cell Biol. 1986;103:2747–54.
15. Carlier M-F, Pantolini D. Direct evidence for ADP-Pi-F-actin as the major intermediate in ATP-actin polymerization. Rate of dissociation of pi from actin filaments. Biochemistry. 1986;25:7789–92.
16. Korn ED, Carlier M-F, Pantaloni D. Actin polymerization and ATP hydrolysis. Science. 1987;238:638–44.
17. Carlier M-F. Role of nucleotide hydrolysis in the polymerization of actin and tubulin. Cell Biophys. 1988;12:105–17.
18. Carlier M-F, Pantolini D. Binding of phosphate to F-ADP-actin and role of F-ADP-P(i)-actin in ATP-actin polymerization. J Biol Chem. 1988;263:817–25.
19. Janmey PA, Hvidt S, Oster GF, Lamb J, Stossel TP, Hartwig JH. Effect of ATP on actin filament stiffness. Nature. 1990;347:95–9.
20. Pollard TD, Goldberg I, Schwarz WH. Nucleotide exchange, structure, and mechanical properties of filaments assembled from ATP-actin and ADP-actin. J Biol Chem. 1992;267:20339–45.
21. Carlier MF, Pantaloni D, Korn ED. The effects of Mg2+ at the high-affinity and low-affinity sites on the polymerization of actin and associated ATP hydrolysis. J Biol Chem. 1986;261(23):10785–92.
22. Graceffa P, Dominguez R. Crystal structure of monomeric actin in the ATP state. Structural basis of nucleotide-dependent actin dynamics. J Biol Chem. 2003;278:34172–80.
23. Reisler E. Actin molecular structure and function. Curr Op Cell Biol. 1993;5:41–7.
24. Elzinga M, Collins JH, Kuehl WM, Adelstein RS. Complete amino-acid sequence of actin of rabbit skeletal muscle. Proc Natl Acad Sci USA. 1973;70:2687–91.
25. Kabsch W, Mannherz HG, Suck D, Pai EF, Holmes KC. Atomic structure of the actin: DNase I complex. Nature. 1990;347:37–44.
26. Szatmári D, Bugyi B, Ujfalusi Z, Grama L, Dudás R, Nyitrai M. Cardiac leiomodin2 binds to the sides of actin filaments and regulates the ATPase activity of myosin. PLoS ONE. 2017;12(10):e0186288.
27. Szatmári D, Xue B, Kannan B, Burtnick LD, Bugyi B, Nyitrai M, Robinson RC. ATP competes with PIP2 for binding to gelsolin. PLoS ONE. 2018;13(8):e0201826.
28. Sanchez-Ruiz JM, Lopez-Lacomba JL, Cortijo M, Mateo PL. Differential scanning calorimetry of the irreversible thermal denaturation of thermolysin. Biochem. 1988;27:1648–52.
29. Jose M. Sanchez-Ruiz. Protein kinetic stability. Biophys Chem. 2010;148:1–15.
30. Mazurenko S, Kunka A, Beerens K, et al. Exploration of protein unfolding by modelling calorimetry data from reheating. Sci Rep. 2017;7:16321.
31. Vyazovkin S. Activation energies and temperature dependencies of the rates of crystallization and melting of polymers. Polymers (Basel). 2010;12:1070.
32. WHO Model List of Essential Medicines. 2015. http://www.who.int/selection_medicines/committees/expert/20/EML_2015_FINAL_amended_JUN2015.pdf?ua=1.
33. Notermans NC, Lokhorst HM, Franssen H, Van der Graaf Y, Teunissen LL, Jennekens FG, Van den Berg LH, Wokke JH. Intermittent cyclophosphamide and prednisone treatment of polyneuropathy associated with monoclonal gammopathy of undetermined significance. Neurology. 1996;47(5):1227–33.
34. Hamidou MA, Belizna C, Wiertlewsky S, Audrain M, Biron C, Grolleau JY. MussiniJM: intravenous cyclophosphamide in refractory polyneuropathy associated with IgM monoclonal gammopathy: anuncontrolled open trial. Am J Med. 2005;118(4):426–30.
35. Kemp G, Rose P, Lurain J, Berman M, Manetta A, Roullet B, Homesley H, Belpomme D, Glick J. Amifostine pretreatment for protection against cyclophosphamide-induced and cisplatin-induced toxicities: results of a randomized control trial in patients with advanced ovarian cancer. J Clin Oncol. 1996;14:2101–12.
36. Spitzer TR, Cirenza E, McAfee S, Foelber R, Zarzin J, Cahill R, Mazumder A. Phase I-II trial of high-dose cyclophosphamide, carboplatin and autologous bone marrow or peripheral blood stem cell rescue. Bone Marrow Transpl. 1995;15:537–42.
37. Tschöp K, Rommel F, Schmidkonz P, Emmerich B, Schulze J. Neuropathy after cyclophosphamide high dose chemotherapy in a Morbus Werlhof patient. Deutsche Med Wsch. 2001;126(12):T17–20.

38. Könczöl F, Wiegand N, Nőt LG, Lőrinczy D. Examination of the cyclophosohamide-induced polyneuropathy on guinea pig sciatic nerve and gastrocnemius muscle with differential scanning calorimetry. J Thermal Anal Calorim. 2014;115:2239–43.
39. Lőrinczy D. Investigation of side effects in polyneuropathy on skeletal muscle by DSC caused by cyclophosphamide treatment. Eur Biophys J. 2019;48(Suppl. 1):S238.
40. Lőrinczy D. Cyclophosphamide treatment evoked side effects on skeletal muscle monitored by DSC. J Thermal Anal Calorim. 2020;142:1897–901.
41. Dergez T, Könczöl F, Farkas N, Belagyi J, Lőrinczy D. DSC study of glycerol-extracted muscle fibers in intermediate states of ATP hydrolysis. J Thermal Anal Calorim. 2005;80:445–9.
42. Dergez T, Lőrinczy D, Könczöl F, Farkas N, Belagyi J. Differenital scanning calorimetry study of glycerinated rabbit psoas muscle fibres in intermediate state of ATP hydrolysis. BMC Struct Biol. 2007;7:41–50.
43. Drewes G, Faulstich H. Cooperative effects on filament stability in actin modified at the C-terminus by substitution or truncation. Eur J Biochem. 1993;212:247–53.
44. Orlova A, Prochniewicz E, Egelman EH. Structural dynamics of F-actin: II. Cooperativity in structural transitions. J Mol Biol. 1995;245:598–607.
45. Orlova A, Egelman EH. Cooperative rigor binding of myosin to actin is a function of F-actin structure. J Mol Biol. 1997;265:469–74.
46. Moracewska J. Structural determinants of cooperativity in actomyosin interactions. Acta Biochim Pol. 2002;49:805–12.
47. Egelman EH. A tale of two polymers: new insights into helical filaments. Nat Rev Mol Cell Biol. 2003;4:621–30.
48. Visegrády B, Lőrinczy D, Hild G, Somogyi B, Nyitrai M. The effect of phalloidin and jaspaklinolide on the flexibility and thermal stability of actin filaments. FEBS L. 2004;565:163–6.
49. Visegrády B, Lőrinczy D, Hild G, Somogyi B, Nyitrai M. A simple model for the cooperative stabilisation of actin filaments by phalloidin and jasplakinolide. FEBS L. 2005;579:6–10.
50. Farkas P, Könczöl F, Lőrinczy D. Examination of the peripheral nerve and muscle damage in cyclophosphamide monotherapy with DSC in animal models. J Thermal Anal Calorim. 2016;126:47–53.
51. Farkas P, Szatmári D, Könczöl F, Lőrinczy D. Cyclophosphamide treatment evoked side effect on skeletal muscle actin, monitored by DSC. J Thermal Anal Calorim. 2021. https://doi.org/10.1007/s10973-021-10774-7.
52. Muzzopappa F, Wilson A, Kirilovsky D. Interdomain interactions reveal the molecular evolution of the orange carotenoid protein. Nat Plants. 2019;5:1076–86.
53. Smock RG, Rivoire O, Russ WP, Swain JF, Leibler S, Ranganathan R, Gierasch LM. An interdomain sector mediating allostery in Hsp70 molecular chaperones. Mol Syst Biol. 2010;6:414.
54. Huang S, Cao J, Jiang M, Labesse G, Liu J, Pin JP, Rondard P. Interdomain movements in metabotropic glutamate receptor activation. Proc Natl Acad Sci USA. 2011;108:15480–5.
55. Vogel M, Mayer MP, Bukau B. Allosteric regulation of Hsp70 chaperones involves a conserved interdomain linker. J Biol Chem. 2006;281(50):38705–11.
56. Guaitoli G, Raimondi F, Gilsbach BK, Gómez-Llorente Y, Deyaert E, Renzi F, Li X, Schaffner A, Jagtap PK, Boldt K, von Zweydorf F, Gotthardt K, Lorimer DD, Yue Z, Burgin A, Janjic N, Sattler M, Versées W, Ueffing M, Ubarretxena-Belandia I, Kortholt A, Gloeckner CJ. Structural model of the dimeric Parkinson's protein LRRK2 reveals a compact architecture involving distant interdomain contacts. Proc Natl Acad Sci USA. 2016;113(30):4357–66.
57. Szatmári D, Lőrinczy D. Alterations of inter domain flexibility in actin monomers reduced by cyclophosphamide treatment. J Thermal Anal Calorim. 2021. https://doi.org/10.1007/s10973-021-11096-4.
58. Kang H, Bradley MJ, McCullough BR, Pierre A, Grintsevich EE, Reisler E, De La Cruz EM. Identification of cation-binding sites on actin that drive polymerization and modulate bending stiffness. Proc Natl Acad Sci USA. 2012;109(42):16923–7.
59. Merino F, Pospich S, Funk J, Wagner T, Küllmer F, Hans-Dieter A, Bieling P, Raunser S. Structural transitions of F-actin upon ATP hydrolysis at near-atomic resolution revealed by cryo-EM. Nat Struct Mol Biol. 2018;25:528–37.
60. Wriggers W, Schulten K. Stability and dynamics of G-actin: backdoor water diffusion and behavior of a subdomain 3/4 loop. Biophysical J. 1997;73:624–39.
61. Scipion CPM, Ghoshdastider U, Ferrer FJ, Yuen TY, Wongsantichon J, Robinson RC. Structural evidence for the roles of divalent cations in actin polymerization and activation of ATP hydrolysis. Proc Natl Acad Sci USA. 2018;115(41):10345–50.
62. Dominguez R, Holmes KC. Actin structure and function. Annu Rev Biophys. 2011;40:169–86. https://doi.org/10.1146/annurev-biophys-042910-155359.
63. Bombardier H, Wong P, Gicquaud C. Effects of nucleotides on the denaturation of F-actin: a differential scanning calorimetry and FTIR spectroscopy study. Biochem Biophys Res Commun. 1997;236:798–803.
64. Emadi A, Jones RJ, Brodsky RA. Cyclophosphamide and cancer: golden anniversary. Nat Rev Clin Onc. 2009;6(11):638–47.
65. Kohn FR, Sladek NE. Aldehyde dehydrogenase activity as the basis for the relative insensitivity of murine pluripotent hematopoietic stem cells to oxazaphosphorines. Biochem Pharm. 1985;34(19):3465–71.
66. Friedman OM, Wodinsky I, Myles A. Cyclophosphamide (NSC-26271)-related phosphoramide mustards- recent advances and historical perspective. Can Treat Rep. 1976;60(4):337–46.
67. Schüller H, Karlsson R, Schutt CE, Lindberg U. Advances in molecular and cell biology. Elsevier. 2006;37:49–61.
68. Orlova A, Shvetsov A, Galkin VE, Kudryashov DS, Rubenstein PA, Egelman EH, Reisler E. Actin-destabilizing factors disrupt filaments by means of a time reversal of polymerization. Proc Natl Acad Sci USA. 2004;101(51):17664–8.